Neuron 50, 883–895, June 15, 2006 ©2006 Elsevier Inc. DOI 10.1016/j.neuron.2006.05.013

Wld^S Protection Distinguishes Axon Degeneration following Injury from Naturally Occurring Developmental Pruning

Eric D. Hoopfer,[1,4] Todd McLaughlin,[2,4] Ryan J. Watts,[1,3] Oren Schuldiner,[1] Dennis D.M. O'Leary,[2,*] and Liqun Luo[1,*]

[1] Howard Hughes Medical Institute
Department of Biological Sciences
and Neurosciences Program
Stanford University
385 Serra Mall
Stanford, California 94305

[2] Molecular Neurobiology Laboratory
The Salk Institute
10010 North Torrey Pines Road
La Jolla, California 92037

[3] Genentech Inc.
1 DNA Way
South San Francisco, California 94080

Summary

Axon pruning by degeneration remodels exuberant axonal connections and is widely required for the development of proper circuitry in the nervous system from insects to mammals. Developmental axon degeneration morphologically resembles injury-induced Wallerian degeneration, suggesting similar underlying mechanisms. As previously reported for mice, we show that Wld^S protein substantially delays Wallerian degeneration in flies. Surprisingly, Wld^S has no effect on naturally occurring developmental axon degeneration in flies or mice, although it protects against injury-induced degeneration of the same axons at the same developmental age. By contrast, the ubiquitin-proteasome system is intrinsically required for both developmental and injury-induced axon degeneration. We also show that the glial cell surface receptor Draper is required for efficient clearance of axon fragments during developmental axon degeneration, similar to its function in injury-induced degeneration. Thus, mechanistically, naturally occurring developmental axon pruning by degeneration and injury-induced axon degeneration differ significantly in early steps, but may converge onto a common execution pathway.

Introduction

Selective pruning of exuberant axons and axon branches occurs widely from insects to mammals and plays an essential role in the proper wiring of the nervous system (Luo and O'Leary, 2005). A major form of developmental axon pruning occurs via degeneration, qualitatively characterized by axon fragmentation and the subsequent removal of fragments by other cells. Axon degeneration was first reported in the large-scale remodeling of the retinotopic map in the optic tectum/superior colliculus (SC) (Nakamura and O'Leary, 1989). Recently, pruning of *Drosophila* mushroom body (MB) γ neuron axons was also demonstrated to occur via degeneration, as shown by axon fragmentation and glial engulfment of axon fragments (Watts et al., 2003, 2004; Awasaki and Ito, 2004). Developmental axon pruning can also be achieved by a distal-to-proximal retraction of the axon. Axon retraction is used in the stereotyped pruning of the infrapyramidal bundle of hippocampal mossy fibers (Bagri et al., 2003; Liu et al., 2005), and has been directly observed for short branches of Cajal-Retzius and thalamocortical axons in the developing cerebral cortex (Portera-Cailliau et al., 2005). In the same study, pruning of long branches of thalamocortical axons was found to occur via degeneration, supporting the general trend that pruning of long portions of primary axons or their collateral branches occurs via degeneration (Luo and O'Leary, 2005). Additionally, synapse elimination at the developing neuromuscular junction in mammals occurs via an "axosome shedding" mechanism: motor axon terminals appear to undergo a distal-to-proximal retraction, but shed membrane-enclosed axosomes at the distal ends, which are engulfed by surrounding Schwann cells (Bishop et al., 2004). Thus, although multiple mechanisms exist, axon degeneration is commonly used for developmental pruning, particularly for longer axon segments.

Axon degeneration during developmental pruning in flies and mammals occurs within a short period of time along the entire length of the axon segments to be pruned (Nakamura and O'Leary, 1989; Watts et al., 2003; Portera-Cailliau et al., 2005). This resembles fragmentation of distal axons in response to axon severing, a process known as Wallerian degeneration (Waller, 1850). Wallerian degeneration is characterized by the rapid breakdown of the cytoskeleton and fragmentation along the entire length of axon segments distal to the injury, usually occurring after a variable waiting period after the initial insult (Griffin et al., 1995). Indeed, the progression of axonal fragmentation occurs with such rapidity that most axons appear either fully intact or completely fragmented at a given time postinjury (Beirowski et al., 2005). Axon fragmentation is followed by a series of responses from surrounding cells, including recruitment of microglia and macrophages to the severed axons (Griffin et al., 1995). These morphological similarities between axon degeneration during developmental pruning and after injury raise the possibility that they share similar mechanisms (Raff et al., 2002).

Studies of Wallerian degeneration slow (*Wld^S*) mice have provided major mechanistic insights into Wallerian degeneration. Compared to the rapid degeneration of severed axons within days in wild-type (wt) mice, *Wld^S* mice exhibit much slower Wallerian degeneration: distal parts of severed axons persist for one to two weeks without obvious signs of fragmentation (Lunn et al., 1989). *Wld^S* is a dominant mutation resulting in the overexpression of a fusion protein of the first 70 amino acids of UFD2/E4, an evolutionarily conserved protein used in protein polyubiquitination, and the full-length

*Correspondence: doleary@salk.edu (D.D.M.O.); lluo@stanford.edu (L.L.)

[4] These authors contributed equally to this work.

nicotinamide mononucleotide adenylyltransferase (Nmnat), an enzyme that facilitates NAD synthesis (Conforti et al., 2000). The effect of *Wld*^{S} is autonomous to injured neurons (Glass et al., 1993), and neuronal expression of Wld^S protein protects against the degeneration of severed distal axons in a dose-dependent manner (Mack et al., 2001). In vitro studies suggest that the Nmnat part of the fusion protein is responsible for its protective effect (Araki et al., 2004; Wang et al., 2005). Remarkably, Wld^S also has protective effects in a variety of disease models, including motor axon "dying back" caused by a tubulin chaperone mutation (Ferri et al., 2003), axon atrophy caused by demyelination (Samsam et al., 2003), axonal spheroid pathology in gracile axonal dystrophy mice (Mi et al., 2005), and axon degeneration in a Parkinson's disease model (Sajadi et al., 2004).

Given its widespread protective effect against injury- and disease-induced axon degeneration, can Wld^S interfere with developmental axon pruning that occurs by degeneration? How similar are the mechanisms involved in axon degeneration during developmental pruning and after injury? Here we report that in *Wld*^{S} mice, pruning of both the retinocollicular and Layer 5 subcortical projections occur normally, indistinguishable from wt mice in the extent and timing. By contrast, Wld^S protects axons of developing retinal ganglion cells (RGCs) from degeneration following complete transection of the optic nerve in the first postnatal week, the same developmental age at which Wld^S has no effect on the naturally occurring developmental degeneration of these same axon projections. We further show that the expression of mouse Wld^S protein has no effect on developmental *Drosophila* MB γ axon pruning, despite its potent effect in protecting fragmentation of severed axons in a *Drosophila* injury model (see also MacDonald et al., 2006, this issue of *Neuron*). By comparing axon degeneration during developmental pruning and after injury, we find that they share similarities in the neuron-intrinsic requirement of the ubiquitin-proteasome system (UPS) and Draper-mediated clearance of degenerating axon fragments by glia, but differ substantially in early steps that trigger axon fragmentation. These data provide insights into both developmental axon pruning and Wallerian degeneration.

Results

Wld^S Does Not Prevent the Developmental Degeneration of RGC Axon Segments during Pruning of the Retinocollicular Projection

In mice, the formation of a retinotopic map in the SC, the major midbrain target of RGC axons, involves the establishment of an initial coarse map, which subsequently undergoes large-scale pruning to generate a refined map (McLaughlin and O'Leary, 2005; Figure 1A). Arbors are established by primary branches that form in a topographically biased manner interstitially along parent RGC axons, all of which overshoot their correct termination zone (TZ) along the anterior-posterior axis of the SC. Previous studies of retinotectal projection development in chicks indicate that the large-scale pruning of overshooting axons and ectopic arbors occurs via degeneration (Nakamura and O'Leary, 1989). We confirmed that the topographic remodeling of the mouse retinocollicular projection also occurs primarily through axon degeneration (Figure 1B).

To compare axon pruning of retinocollicular projections between wt and *Wld*^{S} mice, we focused on the projections of RGCs in temporal retina, because their axons exhibit the greatest overshoot of their appropriate TZ and thus undergo the most substantial amount of pruning. Single, similarly sized, small injections of the anterograde axon tracer DiI were made in similar locations in peripheral temporal retina of wt (Figures 1C–1E) and *Wld*^{S} (Figures 1F–1H) mice between P0 and P7, which are ages that span the postnatal development of the retinocollicular projection. In mice analyzed between P1–P2 (wt, n = 8; *Wld*^{S}, n = 10), we find that essentially all primary RGC axons initially extend posteriorly across the SC, well beyond the correct anterior-posterior location of their future TZ (Figures 1C and 1F, circles; quantified in Figure 1I).

By P3–P4, a substantial degree of remodeling has taken place in both wt (Figure 1D; n = 13) and *Wld*^{S} mice (Figure 1G; n = 15), although a proportion of the original population of overshooting primary RGC axons persists (Figure 1I). By this age, branches of RGC axons have begun to arborize densely around the correct location of their TZ, though they cover a larger domain than at later ages. In wt mice, the large-scale remodeling of the retinotopic map is complete by P7 (Figure 1E; n = 8), where essentially all axon segments beyond the correct TZ have been eliminated, leaving a refined projection characterized by a densely labeled, focal TZ (Figure 1I). We find that the appearance of the projection in P7 *Wld*^{S} mice (Figures 1H and 1I; n = 6) is indistinguishable from that in wt mice at this and earlier ages. Thus, both the initial development and large-scale remodeling of the retinocollicular projection occur in a normal manner in *Wld*^{S} mice.

Wld^S Protects against Injury-Induced Degeneration of Developing RGC Axons

To rule out the possibility that the lack of an effect on naturally occurring developmental axon degeneration of developing RGCs in *Wld*^{S} mice is age-related, we tested whether the injury-induced degeneration of developing RGC axons is protected in *Wld*^{S} mice. We compared in wt and *Wld*^{S} mice the effect of completely transecting RGC axons by unilateral enucleations and analyzed the RGC axon projections during the first postnatal week—the same developmental stage at which naturally occurring degenerative axon pruning of developing RGC axons occurs.

We find that developing RGC axons prelabeled with DiI exhibit rapid degeneration following unilateral enucleations that transect all RGC axons, consistent with previous studies (Pak et al., 2004). In our study, RGC axons were labeled with large DiI injections at P1; the injected eye was either left intact or later removed at P3, and the optic pathway was analyzed at P5 or P7–P8 (Figure 2). When the eye was left intact, RGC axons are well labeled throughout the optic pathway (Figures 2B and 2B′; n = 4). In the unilaterally enucleated cases, residual spots of DiI are seen distributed throughout the region of the optic tract (OT) and SC in wt mice, consistent with debris from the prelabeled RGC axons in the process of degeneration; importantly, we did not observe any

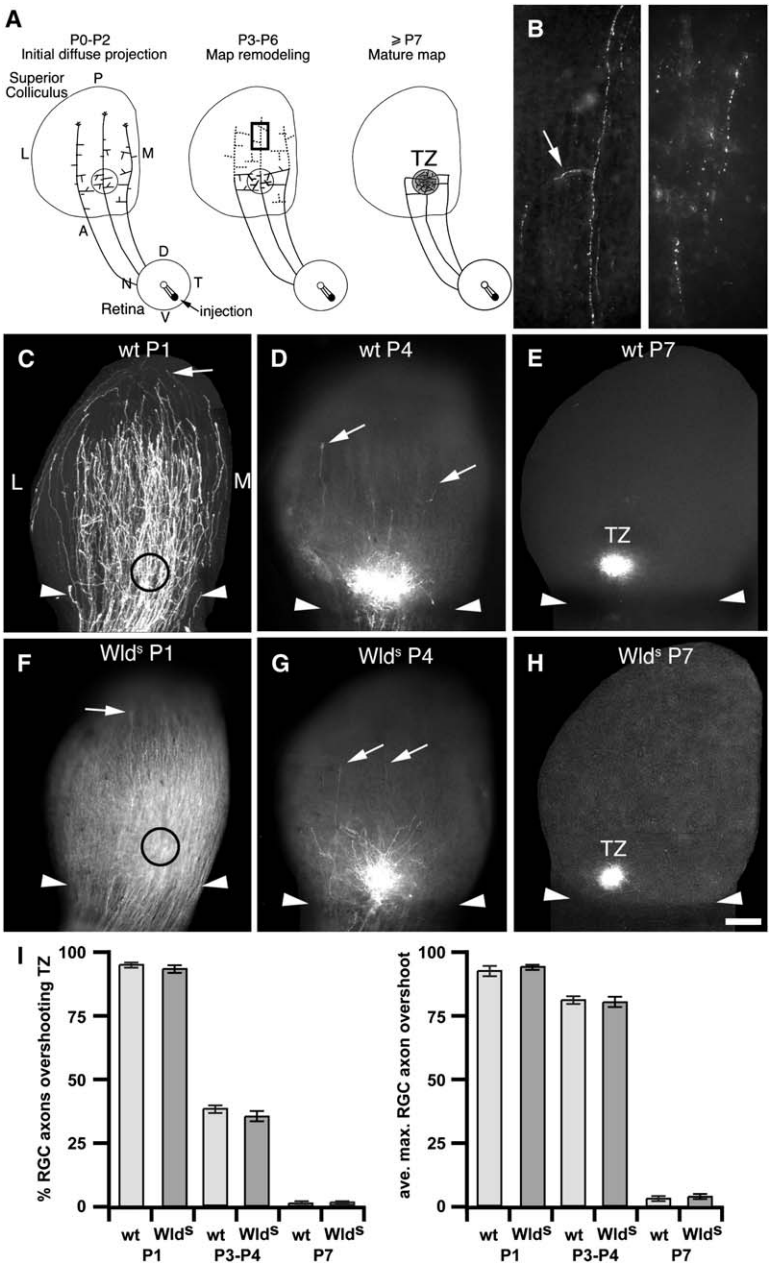

Figure 1. Degenerative Remodeling of the Retinocollicular Projection Is Normal in *Wld*^{S} Mice

(A) Retinal ganglion cell (RGC) axons initially (P0–P2) overshoot their future termination zone (TZ; circle) in the superior colliculus (SC). They then extend branches biased for the anterior (A)-posterior (P) position of their future TZ. Branches extend (P3–P6) to the future TZ and arborize. Inappropriate axon segments are eliminated through degeneration (dotted line axons). Box indicates the location of photos in (B). At P7 a remodeled TZ resembling its mature form is evident. (B) Photomontages of degenerating RGC axons at P3 after focal injection of DiI at P1. RGC axons and interstitial branches (arrow) are discontinuous and fragmented. These images are approximately 1 mm posterior to the nascent TZ. (C–H) Similarly sized and positioned focal injections of DiI in temporal (T) retina in wild-type (wt) (C–E) and *Wld*^{S} (F–H) mice. (C and F) At P1 an initial coarse projection with all RGC axons extending well posterior (arrows) to the future TZ (circle) in anterior SC (arrowheads) in wt (C) and *Wld*^{S} (F) mice. (D and G) By P3–4 the projection refines to a diffuse TZ in anterior SC. Most RGC axons have eliminated overshooting axon segments to the point of a sustaining arbor, though some RGC axons are evident in mid SC and posterior SC (arrows) in both wt and *Wld*^{S} mice. (E and H) At P7 a dense, focal TZ is evident in anterior SC, resembling its mature form. Few RGC axon segments persist in posterior locations in either wt or *Wld*^{S} mice.

(I) (Left) Number of RGC axons present posterior to the future TZ, expressed as a percentage of the total number of RGC axons present at the anterior border of the SC. Error bars indicate SEM. There are no significant differences at any stage between wt and *Wld*^{S} mice (t test, $p > 0.5$). (I) (Right) Average maximum overshoot for RGC axons past the future TZ. Average position of the posterior-most RGC axon growth cone expressed as a percentage of the distance from the posterior edge of the developing TZ to the posterior edge of the SC. Error bars indicate SEM. There are no significant differences at any stage between wt and *Wld*^{S} mice (t test, $p > 0.6$). n for each condition (number of axons and number of animals analyzed, respectively) are as follows: P1: wt (n = 270, n = 4), *Wld*^{S} (n = 310, n = 4); P3: wt (n = 348, n = 6), *Wld*^{S} (n = 488, n = 9); P7: wt (n = 407, n = 8), *Wld*^{S} (n = 296, n = 6).

D, dorsal; L, lateral; M, medial; N, nasal; V, ventral. Scale bars, 10 μm for (B); 300 μm for (C)–(H).

intact RGC axons at 2 days (n = 5) or 4–5 days (n = 3) after unilateral enucleation (Figures 2C, 2C′, and 2F). By contrast, in *Wld*^{S} mice many intact RGC axons and fascicles are present in the SC and OT at both 2 days (Figures 2D and 2D′; n = 5) and 4–5 days (Figure 2E; n = 5) postenucleation, even in the posterior extreme of the SC (Figure 2E′). These qualitative differences indicate that Wld^S protects RGC axon degeneration after injury.

To determine the extent of protection by Wld^S, we quantified the frequency of intact axons in the OT before axons enter the SC, since degenerative pruning of exuberant RGC axon segments does not occur in this area (Figure 2F). We found that in *Wld*^{S} mice there is a significant decrease of intact axons at 4 days compared to 2 days postenucleation; furthermore, DiI-labeled spots are evident in *Wld*^{S} mice after injury (Figures 2D′ and 2E′). Together, these data suggest that Wld^S most likely delays rather then prevents injury-induced axon degeneration during this period.

Wld^S Does Not Prevent Developmental Degeneration of Axon Segments during Pruning of Cortical Layer 5 Projections

We next analyzed the development of Layer 5 projections of the neocortex to their major subcortical targets, focusing on the projections of Layer 5 neurons in visual

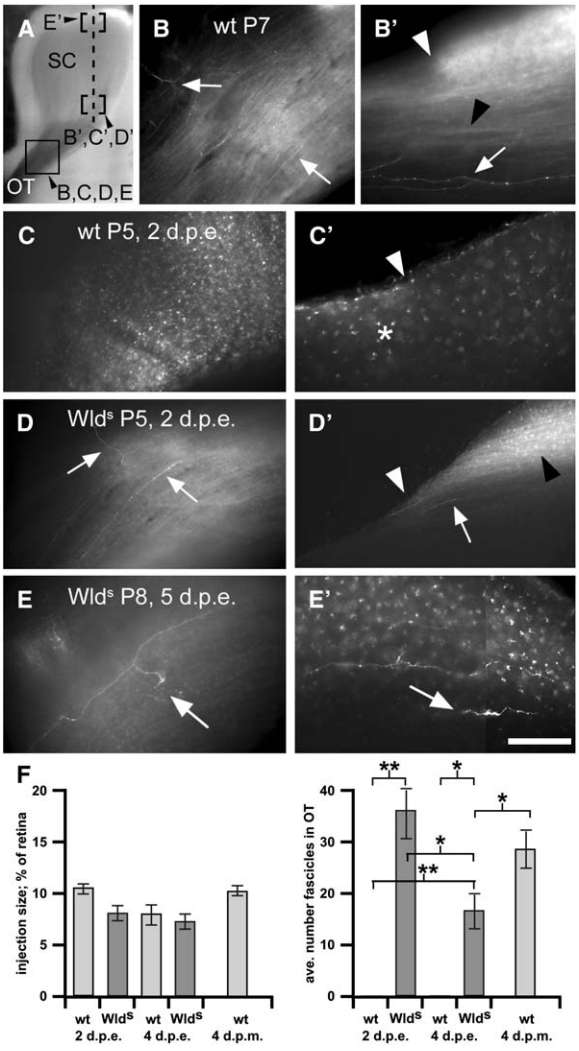

Figure 2. Injury-Induced Axon Degeneration in Developing RGC Axons Is Delayed

(A) Schematic depicts dorsal midbrain; posterior superior colliculus (SC) is at the top, the optic tract (OT) is at the bottom, and the midline is to the right. The optic pathway is delineated by RGC axons (gray) marked with a β-gal reporter (Pak et al., 2004). The box and brackets specify the imaged areas for the indicated panels (dashed line indicates plane of section).

(B) Wt P7 brain after a large injection of DiI at P1; dorsal view of the OT from the intact eye (B) shows fascicles and individual brightly labeled RGC axons (arrows). (B′) Section of the brain in (B) at the anterior border of the SC (white arrowhead) reveals large fascicles (black arrowhead) and individual brightly labeled RGC axons (arrow).

(C–E) Wt (C) and *Wld^s* mouse ([D] and [E]) brains after large injections of DiI into nasal retina at P1, enucleation at P3 of the injected eye, and fixation at the ages indicated. RGC axonal labeling was confirmed in enucleated retinas. (C) At P5 in wt mice, 2 days postenucleation (d.p.e.), spotty labeling reminiscent of large numbers of degenerated axons is seen in the OT. Residual labeling of midbrain cells is visible, but no intact axons are found. (C′) Sections of the brain in (C) at the anterior border of the SC (arrowhead) reveal residual cellular labeling reminiscent of large-scale axonal degeneration (asterisk), with no intact axons. (D) At 2 d.p.e. in *Wld^s* mice, large fascicles of DiI-labeled RGC axons as well as individual well-labeled RGC axons and branches (arrows) are seen in the OT. (D′) Sections of the brain in (D) reveal, in anterior SC (white arrowhead), large fascicles (black arrowhead) and individual well-labeled axons (arrow) similar to the control-labeled wt mice (B′). (E) In *Wld^s* mice at 5 d.p.e., RGC axons and individual brightly labeled RGC axons and branches in the OT (arrow) are evident. (E′) Sections of the brain in (E) reveal, in posterior SC, intact RGC axons and branches (arrow) as well as signs of residual labeling of midbrain cells reminiscent of RGC axon degeneration and DiI fluorescent debris. Sections in panels (B′)–(E′) are 100 μm thick.

(F) (Left) Average DiI injection size, calculated as a percentage of the surface area of the retina. There are no significant differences between wt and *Wld^s* mice within or between conditions (t test, $p > 0.5$). (F) (Right) Average number of fascicles of intact RGC axons present in the optic tract (OT). Error bars indicate SEM. Brackets with single asterisk indicate significance of $p < 0.05$; double asterisks, $p < 0.01$. Abbreviations: d.p.e., days post enucleation; d.p.m., days post mock-enucleation. n for each condition (number of fascicles or axons and number of animals analyzed, respectively): 2 d.p.e.: wt (n = 0 axons, n = 5), *Wld^s* (n = 179 fascicles, n = 5); 4 d.p.e.: wt (n = 0 axons, n = 3), *Wld^s* (n = 81 fascicles, n = 5); 4 d.p.m.: wt (n = 114 fascicles, n = 4).

Scale bars, 1200 μm for (A); 200 μm for (B)–(E); and 100 μm for (B′)–(E′).

cortical areas. During development, all primary Layer 5 axons from visual areas grow well past their posterior-most adult target, the basilar pons, and many extend into the spinal cord (Figure 3A). Later, portions of the primary axon and all of its collateral projections posterior to the basilar pons are eliminated, while the proximal portion of the primary axon, as well as branches to the basilar pons and more proximal targets, are maintained (O'Leary and Terashima, 1988; O'Leary et al., 1990). Previous studies in rats indicate that this pruning of exuberant Layer 5 projections occurs via degeneration (B. Reinoso and D.D.M. O'Leary, 1989, Soc. Neurosci., abstract); we have confirmed this observation in mice (Figure 3B).

We find that the development of Layer 5 projections is indistinguishable between wt and *Wld^s* mice. Injections of DiI were made in comparable locations in the occipital (visual) cortex of wt and *Wld^s* mice at various postnatal ages spanning the development of Layer 5 projections. In P16 mice, the branched projection to the basilar pons is well developed, though many of the primary Layer 5 axons that overshoot this posterior-most target still have axon segments posterior to it in both wt (Figure 3C; n = 4) and *Wld^s* mice (Figure 3D; n = 3) (quantified in Figure 3G). By the end of the third postnatal week (P21–P22), when the Layer 5 projection in wt mice achieves its mature appearance, again the projection patterns are indistinguishable between wt (Figure 3E; n = 3) and *Wld^s* mice (Figure 3F [n = 5] and Figure 3G): all segments of primary Layer 5 axons within the corticospinal tract posterior to the basilar pons are eliminated. These analyses indicate that in *Wld^s* mice the completeness and timing of the large-scale pruning of Layer 5 projections, including the degeneration of several millimeters of primary Layer 5 axons distal to the basilar pons, is indistinguishable from wt mice.

Wld^s Expression Does Not Affect *Drosophila* MB γ Axon Pruning

Developmental pruning of MB γ neuron axons occurs via spatially localized axon degeneration (Watts et al., 2003; Figure 4A). To determine whether Wld^s expression could block pruning of MB γ axons, we made transgenic flies expressing the mammalian Wld^s fusion protein

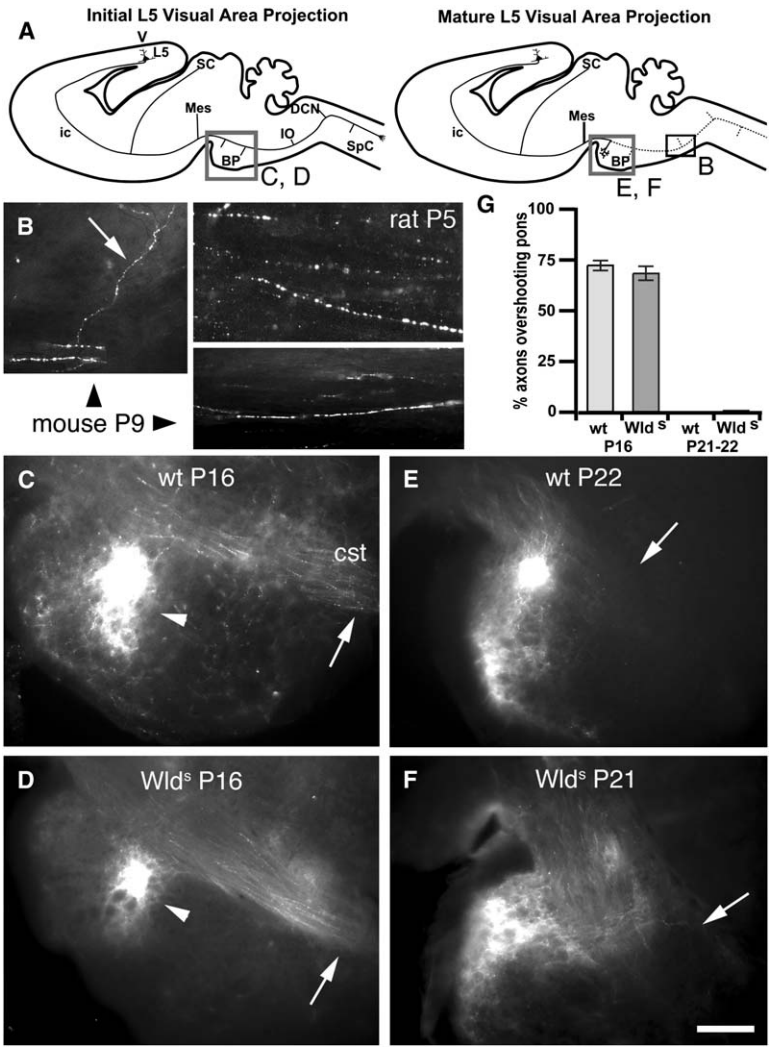

Figure 3. Degenerative Pruning of Layer 5 Subcortical Projections Occurs Normally in *Wld*^{S} Mice

(A) Layer 5 neurons from visual cortex (V) initially project to appropriate targets (i.e., basilar pons [BP]; superior colliculus, [SC]) and inappropriate targets (i.e., inferior olive, [IO]) (left panel; square indicates area shown in panels [C] and [D]). Axon segments to inappropriate targets are later eliminated through degeneration (dashed axons) to the point of a sustaining arbor (right panel; square indicates area shown in [E] and [F]; rectangle indicates area shown in panel [B]). (B) Layer 5 neurons from visual cortex labeled with DiI as they appear posterior to the IO at P9 in mouse (arrowheads) and P5 rat (upper right panel). In both mouse and rat, inappropriate corticospinal axons are discontinuous with many breaks and a fragmented appearance. Branches associated with inappropriate axon segments, such as those to the IO (arrow, left), are eliminated concurrently with the primary axon. (C and D) At P16 in wt (C) and *Wld*^{S} (D) mice, an injection of DiI in visual cortex labels Layer 5 axons with arbors (arrowheads) in the basilar pons (BP). By this age, in both wt and *Wld*^{S} mice, many Layer 5 axons have eliminated their overshooting axon segments to the point of a sustaining arbor, though a proportion of Layer 5 axons are still evident posterior to the BP (arrows) in the corticospinal tract (cst). (E and F) By P21–P22 in wt (E) and *Wld*^{S} (F) mice, an injection of DiI in visual cortex reveals Layer 5 axons innervating the BP. Axon segments posterior to the BP have been eliminated to the point of a sustaining arbor (arrows) in both wt and *Wld*^{S} mice.

(G) Number of cortical Layer 5 axons with segments posterior to the basilar pons at the times indicated, expressed as a percentage of the total number of axons at the anterior border of the pons. There are no significant differences between wt and *Wld*^{S} mice at either age ($p > 0.4$). n for each condition (number of axons and number of animals analyzed, respectively) are as follows: P16: wt (n = 298, n = 4), *Wld*^{S} (n = 218, n = 3); P20: wt (n = 104, n = 3), *Wld*^{S} (n = 188, n = 5). Error bars = SEM.

Abbreviations: DCN, dorsal column nuclei; ic, internal capsule; L5, Layer 5; Mes, mesencephalon; SpC, spinal cord. Scale bars, 20 μm for (B); 150 μm for (C)–(F).

(Mack et al., 2001) under the control of Gal4/UAS. We expressed Wld^S using 201Y-Gal4, which is specifically expressed in γ neurons during larval and early pupal stages. In wt MBs, each larval γ neuron extends two axon branches from the peduncle (Figure 4A), collectively forming a dorsal and a medial lobe (Figure 4B). By 12 hr after puparium formation (12h APF), both axon branches have degenerated up to the peduncle (Figure 4C), leaving behind sparse axon fragments (dashed arrows in Figure 4C), which are mostly cleared by 18h APF (Watts et al., 2003).

Expression of Wld^S in γ neurons does not affect axon growth or branching of larval MB neurons (Figure 4D, compare with Figure 4B), nor does it block γ neuron pruning as evidenced by the extensive fragmentation of γ axons at 12h APF (dashed arrows in Figure 4E). We have performed this experiment with multiple UAS-Wld^S transgenic inserts, multiple copies of the transgene, a stronger MB-Gal4 line OK107, at a higher temperature, and in various combinations of the above, all to increase Gal4-driven transgene expression level—but none of these conditions inhibit MB γ axon pruning (data not shown).

Wld^S Expression Inhibits Axon Degeneration after Injury in *Drosophila*

To address whether mammalian Wld^S has activity in *Drosophila*, we tested whether its expression could protect transected axons from degeneration. The *Drosophila* olfactory circuit provides an ideal system to study axon degeneration due to its well-characterized anatomy and the molecular tools available to label specific subsets of neuronal classes (Berdnik et al., 2006). *Drosophila* olfactory receptor neurons (ORNs), whose cell bodies are located in the antenna and maxillary palp, project axons to the antennal lobe in the central brain. ORNs that express the same olfactory receptor project axons both ipsilaterally and contralaterally to the same glomeruli (Vosshall et al., 2000; Stocker et al., 1990; Figure 5A). In a companion manuscript, MacDonald and colleagues have shown that cutting ORN axons by surgically removing the third antennal segments of the

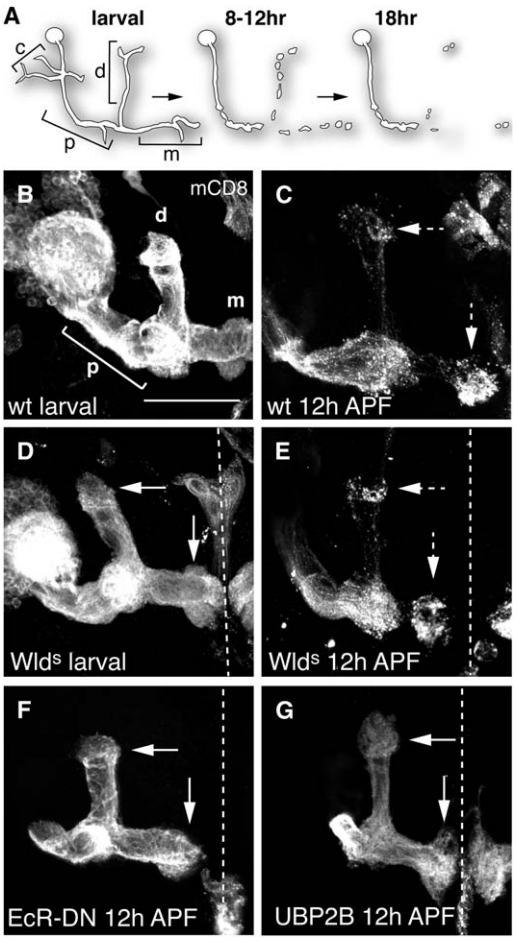

Figure 4. MB γ Neuron Pruning Is Not Affected by Wld^S Expression

(A) Schematic illustrating pruning of a MB γ neuron during metamorphosis. Larval γ neurons have a dorsal (d) and medial (m) axon branch and dendrites in the MB calyx (c). By 18h after puparium formation (APF), dendrites and axons have degenerated back to the primary axon (peduncle, p), which remains intact.

(B and C) Wt γ neurons in third-instar larvae (B) have intact axon lobes, which are mostly pruned by 12h APF ([C], dashed arrows).

(D and E) Expression of Wld^S in γ neurons does not affect axon growth and branching in larvae ([D], arrows), nor does it inhibit pruning of axon branches as shown by axon fragments in 12h APF pupal MB ([E], dashed arrows).

(F and G) MB γ neurons expressing a dominant-negative ecdysone receptor (EcR-DN) (F) or yeast UBP2 (G) show intact axon branches at 12h APF (arrows).

MB γ neuron specific 201Y-Gal4 was used to drive expression of mCD8::GFP and other transgenes; dashed lines delineate the midline. For each experiment, n ≥ 10. Scale bar, 50 μm.

antennae in adult leads to Wallerian-like degeneration of severed axons within 1 day of cutting. Strikingly, expression of the same UAS-Wld^S transgene described above potently delays the degeneration of two examined classes of ORN axons after their cell body removal (MacDonald et al., 2006).

We confirmed and extended these findings in a third class of ORNs by using Or47b-Gal4 to drive expression of a membrane-bound GFP (mCD8::GFP) and various other transgenes (see later). Or47b ORN axons target the VA1lm glomerulus (Vosshall et al., 2000; Figure 5C$_1$). One day after antennae removal, severed wt ORN axons appear fragmented, especially where axons cross the midline (Figure 5C$_2$ and 5C$_2'$). Axons are no longer detectable by 5 or 10 days after severing (Figures 5C$_3$ and 5G; see also Figure S1 in the Supplemental Data), although sparsely dispersed GFP$^+$ fragments are still visible in or around VA1lm. Wld^S expression in Or47b ORNs markedly delays degeneration of severed ORN axons (Figure 5D). No fragmentation is apparent at 1 or 10 days after antennae removal (Figures 5D$_2$, 5D$_2'$, and 5D$_3$), with a thick axon bundle crossing the midline clearly visible in each brain (Figure 5G; Figure S1).

To further confirm the protective effect of Wld^S in injured fly axons, we examined ORN axon degeneration after injury at the ultrastructural level. We expressed the genetically encoded electron microscopy (EM) membrane marker HRP::CD2 (Watts et al., 2004) in Or47b ORNs in the absence or presence of Wld^S coexpression and compared HRP-labeled Or47b commissural axons near the midline before and 1 day after antennae removal (Figure 6). Guided by HRP-labeling visualized in light microscopy, we systematically examined EM sections throughout the ORN axon commissure (equivalent to boxed region in Figure 5C$_1$). In uncut samples (n = 2 flies), intact commissural ORN axon bundles connect the two brain hemispheres—a fraction of which are HRP-labeled, thus representing Or47b ORN axons (Figure 6A). However, in wt flies 1 day after the cut (n = 3) we rarely find intact axons, HRP-labeled or unlabeled, in the area where ORN axons cross the midline (Figure 6B$_1$). In fact, HRP-labeled membranes of any type are rarely found (for one example, see arrowheads in Figure 6B$_2$). Instead, we find clear signs of axon degeneration, such as the presence of multilamellar bodies (MLBs; asterisks in Figure 6B$_2$). Thus, 1 day after cutting, most ORN axons are fragmented and debris appears to be engulfed by neighboring cells, analogous to MB γ axon developmental pruning (Watts et al., 2004). By contrast, when Wld^S is coexpressed with HRP::CD2 in Or47b ORNs (n = 2), intact, labeled ORN commissural axons are abundant 1 day after the cut (Figures 6C$_1$ and 6C$_2$), with intact microtubules evident in some HRP-labeled axon profiles (Figure 6C$_2$, arrowhead). However, these intact axons are in the midst of unlabeled areas containing degenerating profiles such as MLBs (asterisk in Figure 6C$_3$), likely due to degeneration of axons from other classes of ORNs not expressing Wld^S. These findings demonstrate at the ultrastructural level that 1 day after cutting, fragmentation of wt ORN axons at the midline is complete, and that Wld^S expression potently prevents axon fragmentation.

Taken together, these data indicate that expression of mammalian Wld^S fusion protein potently protects degeneration of severed ORN axons in *Drosophila*, but does not affect axon degeneration during developmental pruning of MB γ neurons. The establishment of an axon injury model in *Drosophila* allowed us to further compare axon degeneration during developmental pruning and after injury in the same organism.

Ecdysone Receptor Inactivation Blocks γ Axon Pruning but Not Axon Degeneration after Injury

Developmental pruning of γ neurons requires the cell-autonomous activity of the nuclear hormone receptor complex composed of the ecdysone receptor isoform

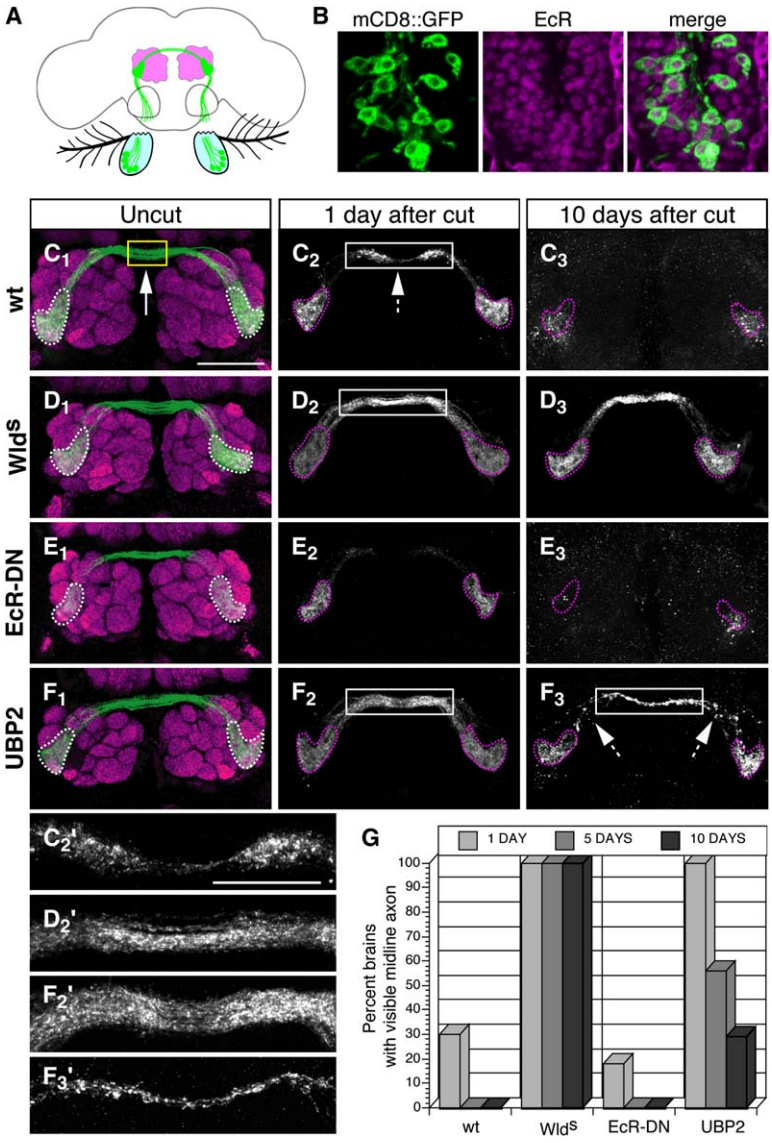

Figure 5. Effect of Various Manipulations on Wallerian Degeneration of ORN Axons after Injury

(A) ORNs expressing Or47b (in green) have cell bodies in the third antennal segment (blue) and project axons to the antennal lobes in the brain (magenta), where they target to the ipsilateral and contralateral VA1lm glomerulus, forming a commissural axon bundle. Removal of both third antennal segments severs ORN axons, and degeneration of their projections in the antennal lobe can be observed.

(B) Immunostaining of adult antennal sections with an antibody against ecdysone receptor (EcR, magenta) shows widespread expression of EcR in ORN nuclei, including Or47b ORNs.

(C–F) Degeneration of severed ORN axons after injury. Wt uncut Or47b ORNs (C_1) show intact axon projections to VA1lm glomeruli (dashed outline) and a thick bundle of commissural axons (solid arrow). Uncut Or47b ORNs expressing Wld^S (D_1), EcR-DN (E_1), or UBP2 (F_1) are similar to wt (C_1). Degeneration of severed wt or EcR-DN-expressing ORN axons is evident 1 day ([C_2] and [E_2]) or 10 days ([C_3] and [E_3]) after cut, with a high-magnification view ([C_2']; rectangle indicates magnified region) showing fragmentation of commissural axons at 1 day after cut. Severed Wld^S axons persist 1 day ([D_2] and [D_2']) and 10 days (D_3) after antennae removal. Expression of UBP2 delays axon degeneration at 1 day ([F_2] and [F_2']) and 10 days (F_3) after axon severing. However, a high-magnification view of severed axons at 10 days (F_3') shows increased fragmentation.

(G) Quantification of ORN axon degeneration. Progression of axon degeneration at 1, 5, and 10 days after antennae removal was quantified by calculating the percentage of brains for each genotype in which contralateral axon projections could still be detected. (See Figure S1 for additional quantifications.) Or47b-Gal4 was used to label ORN axons with mCD8::GFP (green) and express specified transgenes. Glomeruli of the antennal lobe were visualized by staining for the presynaptic marker nc82 (magenta), and VA1lm glomeruli were traced from corresponding stacks (dashed lines). For each genotype's uncut experiment, n > 10. The number of brains for each time point (1, 5, and 10 days, respectively) is as follows: wt (23, 20, 19); *Wld*^{S} (16, 13, 16); *EcR-DN* (22, 27, 20); *UBP2* (15, 27, 35). Scale bar, 50 μm for (C)–(F); 25 μm for (C_2'), (D_2'), (F_2'), and (F_3').

B1 (EcR-B1) and Ultraspiracle (USP), the *Drosophila* homolog of the mammalian retinoic acid receptor (Lee et al., 2000). Expression of dominant-negative ecdysone receptor (EcR-DN; Cherbas et al., 2003) in γ neurons using 201Y-Gal4 strongly inhibits axon pruning (Figure 4F; Awasaki and Ito, 2004). Ecdysone/EcR appears to be a general regulator of developmental pruning during *Drosophila* metamorphosis, as cell-autonomous blockade of ecdysone signaling inhibits developmental pruning of neuropeptidergic neurons in the ventral nerve cord (Schubiger et al., 2003), persistent olfactory projection neurons (Marin et al., 2005), and sensory neurons (Kuo et al., 2005; Williams and Truman, 2005).

Is ecdysone/EcR also essential for axon degeneration after injury? We found that adult ORNs express ecdysone receptor and are thus capable of mediating ecdysone signaling (Figure 5B). To determine if ecdysone signaling is required for the degeneration of severed ORN axons, we expressed UAS-EcR-DN in Or47b ORNs. Axon morphology and targeting of Or47b ORNs expressing EcR-DN is normal (Figure 5E_1). In contrast to its effects on MB γ neuron pruning, expression of EcR-DN in ORNs does not prevent degeneration of severed axons (Figure 5E; quantified in Figure 5G and Figure S1). These data indicate that ecdysone signaling, which initiates developmental pruning of MB γ neurons, is not required for degeneration of axons after severing.

UPS Inhibition Interferes with MB γ Axon Pruning and ORN Axon Degeneration after Injury

Previously we have shown that the ubiquitin-proteasome system is required cell-autonomously for axon pruning (Watts et al., 2003). In particular, expression of the yeast deubiquiting enzyme UBP2, which removes

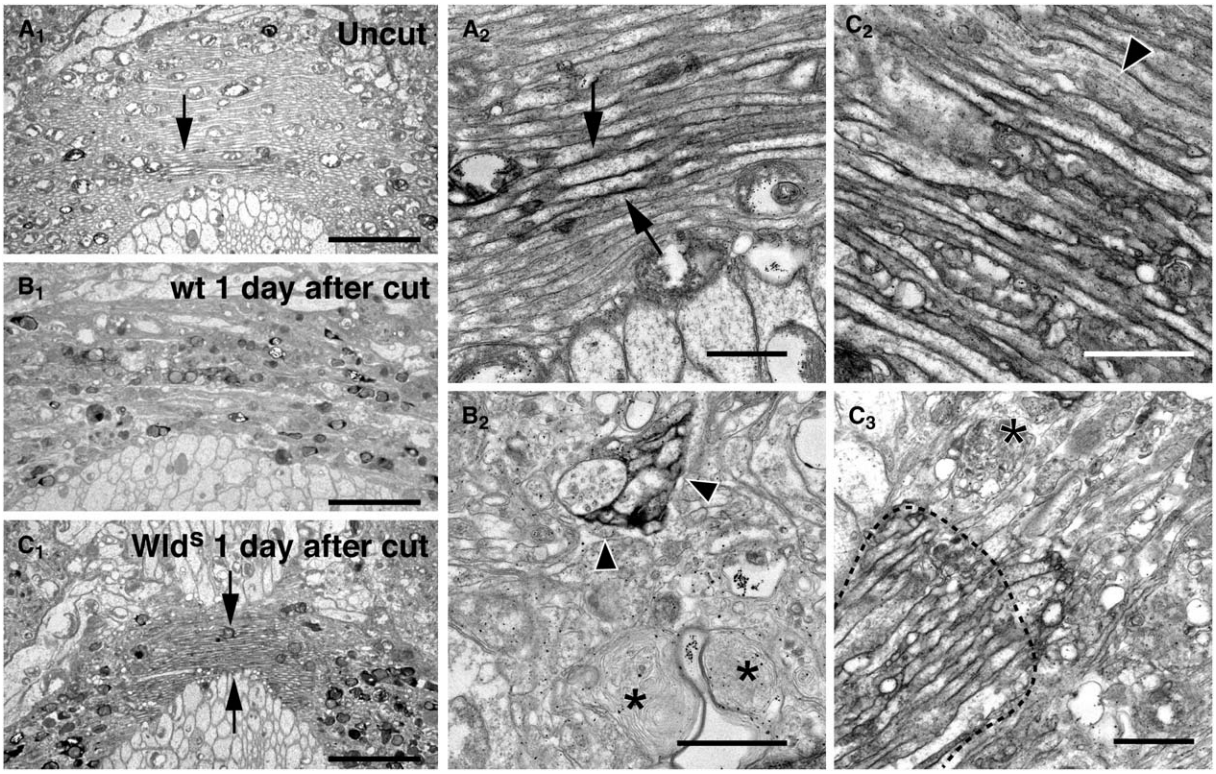

Figure 6. Ultrastructural Analysis of ORN Axon Degeneration after Injury

(A) Ultrastructure of ORN axons at the commissure in uninjured fly brains. (A_1) Low magnification of ORN commissural axons at the midline (region shown is indicated by yellow box in Figure 5C_1) shows longitudinal sections of axons. Electron dense deposits mark the membranes of intact Or47b ORNs visualized by HRP::CD2 expression (arrow), surrounded by intact but unlabeled ORNs of other classes. (A_2) High magnification of a subset of labeled intact axons (arrows), surrounded by unlabeled ORN axons.

(B) Wt ORN axons (with Or47b axons expressing HRP::CD2) 1 day after cutting. (B_1) Low magnification of an analogous area as in (A_1) shows highly disorganized ultrastructure of wt commissural axons that is indicative of degeneration. (B_2) High magnification of the commissural axons at the midline shows a lack of intact axons. Signs of axon degeneration are evident, such as multilamellar bodies (MLBs, asterisks) and few remaining labeled membranes (arrowheads). (Note: darkly labeled circular structures in low-magnification views are mitochondria, which cross-react in the HRP substrate reaction.)

(C) Wld^S-expressing ORN axons 1 day after cutting. (C_1) Low magnification shows a bundle of intact HRP-labeled axons (arrows) crossing the midline, surrounded by degenerating axon debris. (C_2) High magnification micrograph showing HRP-labeled axons that contain microtubules (arrowheads). (C_3) HRP-labeled intact axons (dashed outline) can be seen adjacent to unlabeled regions that appear highly disorganized and contain unlabeled MLBs (asterisk).

Scale, 2 μm for (A_1)–(C_1); 1 μm for (A_2)–(C_3).

ubiquitin from a subset of tagged substrates, inhibits axon pruning of MB γ neurons, as evidenced by the intact axon branches at 12h APF (Figure 4G, compare with Figure 4C), which persist into adulthood (Watts et al., 2003). Expression of UBP2 also inhibits dendritic pruning of sensory neurons (Kuo et al., 2005), suggesting a general role of the UPS in diverse developmental pruning paradigms in *Drosophila*.

We expressed UBP2 in Or47b ORNs to test its effect on axon degeneration after injury. Or47b ORNs expressing UBP2 appear morphologically indistinguishable from wt neurons prior to axon severing (Figure 5F_1). One day after severing, UBP2-expressing ORNs show little signs of degeneration (Figure 5F_2). They still form a thick and continuous tract of commissural axons (Figure 5F_2'), which appear qualitatively more similar to Wld^S-expressing ORN axons (Figure 5D_2') than to the fragmented wt axons (Figure 5C_2'). UBP2-expressing axons are still visible 10 days after severing (Figure 5F_3); however, axon fragments are now apparent (dashed arrows) and the commissure appears thin and fragmented (Figure 5F_3'). We quantified the number of brains in each experimental condition in which we could detect commissural axons, regardless of the thickness of the remaining tract (Figure 5G). We also quantified fluorescence intensity of residual axons at the midline after antennae removal (Figure S1). Both analyses indicate that UBP2 has a similar protective effect as Wld^S 1 day after the cut; however, the protective effect of UBP2, although still significant, is much less pronounced than that of Wld^S at 5 and 10 days after the cut. Thus, UBP2 expression delays axon degeneration, albeit to a lesser extent than Wld^S expression.

Efficient Clearance of γ Neuron Axon and Dendrite Fragments Requires Draper

At a late phase of MB γ axon pruning, axon fragments are engulfed by glia, likely for endosome-lysosome mediated degradation (Watts et al., 2004; Awasaki and Ito, 2004). In an accompanying manuscript, ORN severing is shown to induce a robust glial reaction around the

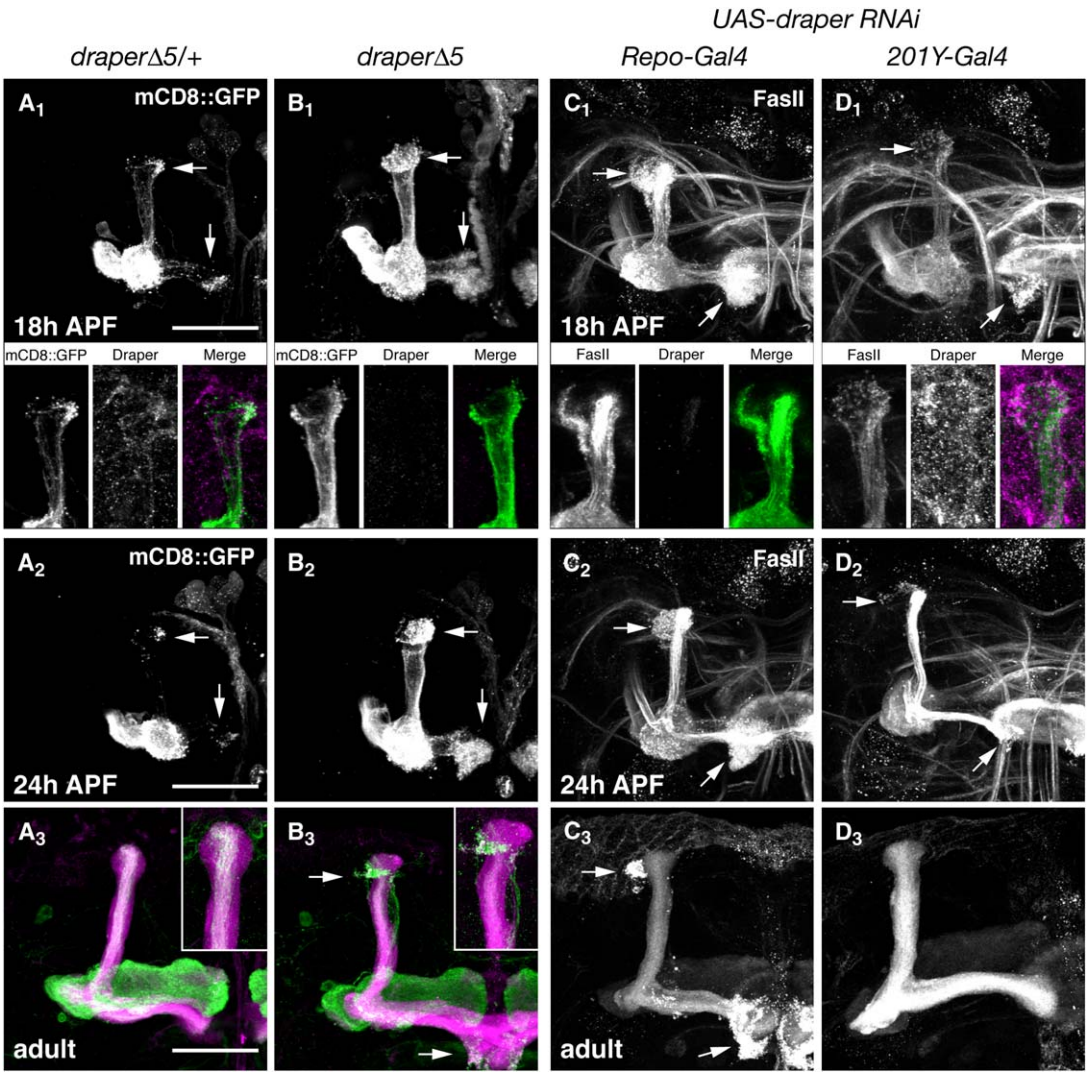

Figure 7. Draper in Glia Is Required for Timely Clearance of Axon Fragments

(A and B) Developmental time course of MB γ axon pruning in control flies ([A]; $drpr^{\Delta 5}$/+) or *draper* mutants ([B]; $drpr^{\Delta 5}/drpr^{\Delta 5}$). *Draper* mutants show more GFP-labeled γ axons and axon fragments (arrows) at both 18h ([B_1]; n = 12) and 24h ([B_2]; n = 18) APF compared with controls ([A_1] and [A_2], respectively; n > 50 for both) (see Figure S2 for quantification). Insets below (A_1) and (B_1) are close-up views of the dorsal lobe showing Draper protein staining surrounding γ axons labeled with mCD8::GFP at 18h APF. Axon fragments (arrows) are visible in *draper* mutant adults 1–2 days after eclosion ([B_3]; n = 12), but have been cleared in control animals ([A_3]; n = 44). In the normal adult, 201Y-Gal4 labels γ neurons, which only make projections to the medial lobe, and a subset of α/β neurons, contributing to the central core of the dorsal α lobe (insets in [A_3] and [B_3]). The entire dorsal α lobe is strongly stained with FasII (magenta).

(C–D) RNAi knockdown of Draper in glia (C) but not in MB γ neurons (D) delays clearance of axon fragments, similar to whole animal *draper* null mutants. Insets show Draper protein expression surrounding the dorsal lobe at 18h APF. Draper expression is strongly reduced when *draper* is knocked down in glia compared with γ neurons (insets in [C_1] and [D_1], respectively). Glial knockdown of Draper results in extensive FasII-labeled axon fragments remaining at 18h and 24h APF ([C_1] and [C_2], respectively; n = 24 and n = 20), as compared with normal axon pruning in γ neuron knockdown ([D_1] and [D_2], respectively; n = 24 and n = 13). In young adult flies, FasII-labeled axon fragments are apparent at the tips of the dorsal and medial lobes in glial (arrows in [C_3]; n = 14), but not γ neuron ([D_3]; n = 7) knockdown of Draper.

Quantifications are shown in Figure S2. Scale bar, 50 μm.

antennal lobes and to recruit Draper to glial membranes near the axon fragments (MacDonald et al., 2006). Draper is the *Drosophila* homolog of *C. elegans* CED-1, a cell-surface receptor required for cell corpse engulfment (Zhou et al., 2001; Freeman et al., 2003). Clearance of severed axon fragments is defective in homozygous *draper* mutant flies (MacDonald et al., 2006). These findings raise the possibility that axon degeneration during developmental pruning and after injury may share similar clearance mechanisms mediated by glia.

To test the function of Draper in MB γ axon pruning, we first compared pruning in *draper* heterozygous versus homozygous animals (Figures 7A and 7B). The null allele ($drpr^{\Delta 5}$; Freeman et al., 2003) is predicted to eliminate protein expression, which is supported by antibody staining in the insets of Figure 7 and quantified in Figure S2. In control brains, the majority of γ axon branches are pruned by 18h APF, with some fragments left at the tips of the axon lobes (Figure 7A_1). By 24h APF, axon pruning is mostly complete (Figure 7A_2).

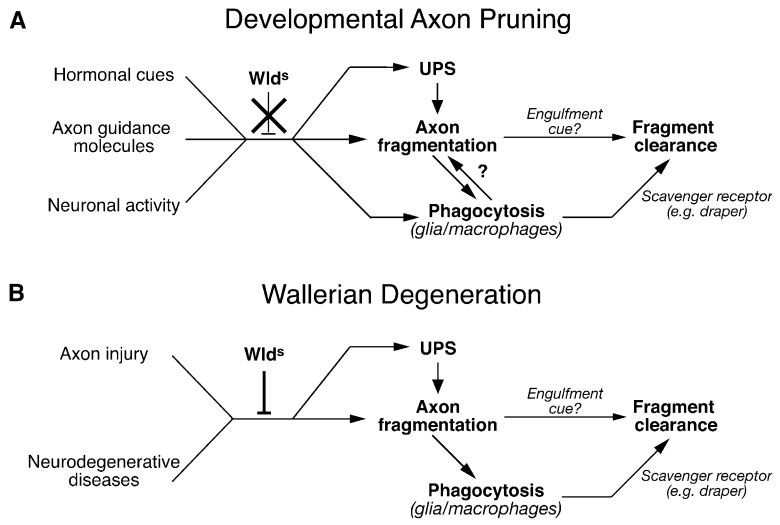

Figure 8. Comparing Axon Degeneration during Developmental Pruning and after Injury

(A) Schematic summary of mechanisms of axon degeneration during developmental pruning. Data are primarily derived from studies of *Drosophila* MB γ axon pruning (Lee et al., 2000; Watts et al., 2003, 2004; Awasaki and Ito, 2004; this study), but aspects also apply to other developmental pruning paradigms (Schubiger et al., 2003; Marin et al., 2005; Williams and Truman, 2005; Kuo et al., 2005).

(B) By comparison, axon degeneration in response to injury or as a result of degenerative diseases differ in their triggers and early steps leading to axon fragmentation, as indicated by their different responses to Wld^S expression. The execution steps, including axon fragmentation and fragment engulfment by phagocytic cells (MacDonald et al., 2006; this study), appear to be shared.

By contrast, in $drpr^{\Delta 5}$ homozygous mutants, there is a marked increase of GFP-labeled fragments at the tips of the axon lobes at 18h and 24h APF (Figures $7B_1$ and $7B_2$; quantified in Figure S2). This defect in fragment clearance is also evident in the calyx, where many dendrite fragments remain in all *draper* mutants examined at 18h APF (Figure S2C), as compared to control animals in which no fragments remain (Figure S2D). By contrast, γ neurons expressing EcR-DN maintain intact axons and dendrites at 18h APF with no fragments detectable (Figure 4F and Figure S2E). In *draper* mutants, some residual γ axon fragments even persist into the young adult (arrows in Figure $7B_3$; compare insets in Figures $7B_3$ and $7A_3$).

Draper has been reported to be expressed predominantly in glia (Freeman et al., 2003), including those that infiltrate MB γ axon segments (Awasaki and Ito, 2004). We expect that glial but not neuronal inhibition of Draper function is responsible for this fragment clearance defect. To confirm this prediction, we expressed UAS-*draper* RNAi specifically in glia or MB γ neurons using pan-glial Repo-Gal4 or 201Y-Gal4, respectively (Figures 7C and 7D). Glial expression of UAS-*draper* RNAi drastically reduced the Draper protein expression in the brain compared to γ neuron knockdown of Draper (insets of Figures $7C_1$ and $7D_1$; Figure S2). We then examined the effect of glial or neuronal knockdown of Draper on MB γ axon pruning by following FasII staining. In early pupae, FasII is expressed in MB γ neurons that undergo axon pruning, but not in α′/β′ neurons, which do not undergo pruning; it is also highly expressed on axons of pupal-born α/β neurons (Lee et al., 1999). Neuronal inhibition of Draper function did not result in any defects at 18h or 24h APF, or in adults (Figure 7D; compare Figure $7D_3$ with magenta in Figure $7A_3$). By contrast, glial inhibition of Draper resulted in a marked increase of FasII-positive axon fragments (arrows in Figures $7C_1$–$7C_3$). These axon fragments are similar in appearance and location to those found in *draper* homozygous null animals (compare Figure 7C and 7B). Taken together, these results demonstrate that *draper* acting in glia is required for the timely clearance of MB γ neuron dendrite and axon fragments.

Discussion

A major cellular mechanism used in naturally occurring developmental pruning of axons from insects to mammals is the localized degeneration of inappropriate axon segments, which morphologically closely resembles injury-induced Wallerian degeneration of axons in adults. We show here that these two processes share some molecular mechanisms as well: they both depend on UPS action in neurons and axon fragment clearance by the cell corpse engulfment receptor Draper in glia. However, our analysis also revealed fundamental differences between developmental and injury-induced axon degeneration. Whereas expression of Wld^S protein potently delays axon degeneration after injury in adult flies and in both developing and adult mice, it does not affect axon degeneration in three developmental axon-pruning paradigms in either organism. We propose that axon degeneration during developmental pruning and after injury differ in the early steps leading to axon fragmentation but may later converge onto a common pathway (Figure 8).

Common Features of Developmental Axon Pruning and Wallerian Degeneration

Beyond the morphological features of axon fragmentation and engulfment of fragments by extrinsic cells, axon degeneration during developmental pruning and after injury share additional similarities. Both processes require cell-autonomous programs, neither requires caspase-dependent apoptotic machinery, and microtubule fragmentation/disappearance is an early sign of axon degeneration in both cases (Raff et al., 2002; Watts et al., 2003; Zhai et al., 2003). By systematically comparing developmental and injury-induced axon degeneration in *Drosophila*, we find additional mechanistic similarities that likely extend to vertebrate systems (compare Figures 8A and 8B).

UPS in Axon Degeneration

MB γ axon pruning requires the intrinsic activity of the UPS (Watts et al., 2003). We now find that UPS inhibition significantly delays injury-induced axon degeneration. At least at early stages, UPS inhibition appears to

delay axon fragmentation (Figure 5F$_2$). This is similar to an in vitro Wallerian degeneration model in mammals, in which inhibition of UPS by application of a proteasome inhibitor or expression of UBP2 delays axon fragmentation (Zhai et al., 2003). These studies suggest that UPS action in facilitating axon fragmentation after injury is a conserved feature from flies to mammals.

Although UPS inhibition can block developmental axon pruning completely under appropriate conditions (Watts et al., 2003), it cannot prevent injured axons from eventual degeneration (Figures 5F$_3$ and 5G; Figure S1). One possible explanation for this difference could be because of the short window of time in which developmental pruning occurs: if pruning is delayed beyond this "critical period," neurons may no longer be in a competent state to carry out the degenerative pruning program. Consistent with this notion is the recent finding of a critical period for large-scale axon degeneration of the retinocollicular projection coincident with the brief time window during which the projection normally undergoes pruning (McLaughlin et al., 2003). In the case of Wallerian degeneration after complete axon transection, since the injury physically separates the axons from their cell bodies, the most that can be done is to prolong the inevitable onset of fragmentation of the already severed axon. However, many neurodegenerative disease models exhibit Wallerian-like axon degeneration, which can be ameliorated by Wld^S expression (see Introduction). Thus, understanding the mechanisms that trigger axon fragmentation may lead to therapeutic strategies to stop axon degeneration before it begins.

Glial Clearance of Axon Fragments

In an accompanying manuscript, MacDonald and colleagues demonstrate a role for glia in the clearance of axon fragments in a *Drosophila* model of Wallerian degeneration. In particular, they identify a requirement of the cell corpse engulfment receptor Draper in glia for this function (MacDonald et al., 2006). We find that removal of Draper in glia markedly delays clearance of axon fragments during MB axon pruning. In addition, ultrastructural analysis of degenerating axons after injury reveals degenerating profiles similar to what we find during MB axon pruning (Watts et al., 2004). These similarities strongly suggest that mechanisms for this late phase of axon degeneration and clearance are shared between developmental pruning and Wallerian degeneration (Figures 8A and 8B).

Glial function has not been systematically explored in developmental axon pruning in mammals. However, the transient appearance in early postnatal cats of clusters of macrophages contiguous to the corpus callosum during the period of callosal axon pruning (Innocenti et al., 1983a, 1983b) suggests that these cells might serve a phagocytic function in vertebrate developmental axon pruning analogous to that of Draper-expressing glia in flies.

Wld^S Protection Distinguishes Mechanisms of Axon Degeneration during Developmental Pruning and after Injury

An important finding of this study is that developmental axon degeneration and Wallerian degeneration can be clearly distinguished mechanistically by their differential sensitivity to the protective effect of Wld^S. Remarkably, this mouse fusion protein can also potently protect axon degeneration after injury in flies. Despite the phylogenetically conserved function of Wld^S in protecting injured axons, we show in three diverse developmental degeneration paradigms in mice and flies that Wld^S expression has no effect on naturally occurring developmental axon pruning. In particular, we show that the injury-induced degeneration of transected RGC axons is markedly protected in *Wld^S* mice at the same age when naturally occurring degenerative pruning of the same developing RGC axons is not protected. This finding demonstrates unequivocally the fundamental difference between axon degeneration during developmental pruning and after injury in the same type of neuron at the same developmental stage. Similarly, Wld^S protects young motor axons from degeneration after injury while having no effect in the remodeling of neuromuscular junction (Parson et al., 1997), although such remodeling uses a distinct mechanism (see Introduction).

What might be the reasons behind this difference between developmental and injury-induced axon degeneration? The trigger for naturally occurring developmental axon degeneration and injury-induced Wallerian degeneration differs, as do their respective roles. Wallerian degeneration is triggered extrinsically by axonal insult. Because degeneration is restricted to the portion of the axon distal to the injury site, it must be executed without new transcription or transport from the cell body. These properties suggest that the effectors of the program are continuously present along the entire length of axons. The function of Wallerian degeneration could be to remove the damaged axons as a step in facilitating regeneration and repair.

In contrast to Wallerian degeneration, the role of developmental axon degeneration is to remodel initially exuberant neuronal connections into a functionally appropriate adult circuit. It is likely triggered by diverse mechanisms including cell-autonomous transcriptional regulation, patterned neuronal activity, the local environment of the axon, or their combination (Figure 8A). For example, MB γ axon pruning is triggered by activation of the steroid hormone receptor EcR to cell-autonomously regulate gene expression (Lee et al., 2000). In the case of the retinocollicular projection, spatial control of pruning is instructed by the distribution and levels of EphA receptors along the length of RGC axons, which is controlled in part by transcriptional regulation autonomous to the RGC. Non-RGC autonomous mechanisms, including the level of ephrin-As to which an RGC axon segment is exposed within the target and correlated patterns of RGC activity generated by networks of RGCs and cholinergic amacrine cells that produce spontaneous retinal waves, are also essential factors for the pruning of inappropriate axon segments (McLaughlin and O'Leary, 2005).

It remains a future challenge to investigate mechanistically how diverse triggers in developmental pruning, injury, and disease lead to similar late stage execution of axon degeneration. Our findings of both a differential effect of Wld^S in these processes and similar roles for the intrinsic activity of UPS and glial clearing of fragmented axons provide an essential step toward this goal.

Experimental Procedures

Axon Tracing and Enucleations in Mice

Wld^{S} mice (CJ57/Bl6 background) were purchased from Harlan (UK) and genotyped as described (Samsam et al., 2003). Labeling and analyses of the retinocollicular projection and cortical Layer 5 projections were done as described by McLaughlin et al. (2003) and O'Leary and Terashima (1988), respectively. Briefly, focal injections of DiI (Molecular Probes) were made into temporal retina and confirmed in retinal wholemounts. After fixation with 4% paraformaldehyde (PF), sections of the SC were cut at 100 μm on a vibratome and analyzed. DiI injections were made into occipital cortex, and later the mice were fixed as above; sections were cut at 100 μm on a vibratome and examined for distribution of labeled axons and to verify that the injections were appropriately restricted. Cases examined for evidence of degeneration were perfused with chilled 4% PF and 10% sucrose in PBS to protect against artifactual beaded axonal morphology (Portera-Cailliau et al., 2005). Enucleations were done as described by Pak et al. (2004). Injections of DiI, substantially larger than those shown in Figure 1, were made into nasal retina, and the injected eye was either left intact or removed 2 days later. Enucleated eyes were removed completely, thereby assuring transection of all RGC axons, and examined for fluorescently labeled RGC axons. Only cases with substantial numbers of labeled RGC axons were processed further. Quantification of overshooting RGC axons in SC, as well as axons in the enucleation experiments, was performed on dorsal views of wholemounts blind to genotype and condition. In some cases sagittal vibratome sections were analyzed to determine maximum posterior overshoot. Quantification for the corticospinal tract (cst) was performed on two randomly selected vibratome sections for each case and examined blind to genotype and age. Layer 5 axons were counted at the anterior and posterior edges of the pons. Axons and injection sizes were quantified in Adobe Photoshop and NIH Image. In most cases images were digitally manipulated to maximize the signal.

Transgenic Flies

For expression of UAS transgenes in MB γ neurons, Or47b ORNs, or glia, we used 201Y-Gal4, Or47b-Gal4, or Repo-Gal4, respectively. The following transgenic lines were used: *UAS-mCD8::GFP* (to label neurons in all experiments for light microscopy), *UAS-HRP::CD2* (for EM), *UAS-EcR-W650A* (Cherbas et al., 2003), *UAS-UBP2B* (DiAntonio et al., 2001), and *UAS-Wld*^{S}.

The Wld^{S} coding sequence (from a plasmid kindly provided by M. Coleman) was PCR amplified with primers designed to add a consensus *Drosophila* Kozak sequence upstream of the start codon and flank the gene with EcoRI and XbaI restriction sites, which were used for cloning into the pUAST vector. The primers are as follows: 5′-GGAATTCGCCGCCACCATGGAGGAGCTGAGCGCTGA-3′ and 5′-GCTCTAGATCAGCGCTCAGCTCCTCCAT-3′. Transgenic flies were generated by standard procedures.

The *drpr*$^{\Delta 5}$ mutant (Freeman et al., 2003) and UAS-*draper* RNAi (MacDonald et al., 2006) was kindly provided by M. Freeman.

Fly Immunostaining and Electron Microscopy

Fly brains were dissected, fixed, and processed for wholemount immunostaining as previously described (Lee and Luo, 1999). For immunostaining of adult antennal ORNs for ecdysone receptor, antennae were cryosectioned at 12 μm and processed as described by Stockinger et al. (2005). The following antibodies were used: rat monoclonal anti-mouse CD8 α subunit, 1:100 (Caltag); mouse monoclonal 1D4, 1:50 (Developmental Studies Hybridoma Bank), mouse monoclonal anti-nc82, 1:30 (kind gift of E. Buchner, U. of Wuerzberg); mouse monoclonal anti-rat CD2 (MCA154G), 1:50 (Serotec, Oxford, UK); mouse monoclonal anti-EcR-C (Ag10.2), 1:10 (Developmental Studies Hybridoma Bank); rabbit polyclonal anti-Draper preabsorbed against *w* embryos, 1:500 (kind gift of M. Freeman, U. of Massachusetts). Electron microscopy labeled with genetically encoded HRP::CD2 marker was performed as previously described (Watts et al., 2004).

Supplemental Data

The Supplemental Data for this article can be found online at http://www.neuron.org/cgi/content/full/50/6/883/DC1/.

Acknowledgments

We particularly thank M. Freeman for communicating unpublished results, sharing reagents, and coordinating publications. We thank K. Yee, T. Komiyama, and M. Cohen for helpful advice and discussion and J. Coble for his contributions; M. Coleman for the plasmid encoding the Wld^{S} fusion protein; H. Su and J. Perrino for technical assistance; and B. Barres, S. McConnell, and members of our labs for comments on the manuscript. E.D.H. is an NSF predoctoral fellow. L.L. is an HHMI investigator. Supported by NIH grants R37-NS041044 (L.L.) and R01-EY07025 and R37-NS31558 (D.D.M.O'L.).

Received: November 14, 2005
Revised: March 30, 2006
Accepted: May 17, 2006
Published: June 14, 2006

References

Araki, T., Sasaki, Y., and Milbrandt, J. (2004). Increased nuclear NAD biosynthesis and SIRT1 activation prevent axonal degeneration. Science *305*, 1010–1013.

Awasaki, T., and Ito, K. (2004). Engulfing action of glial cells is required for programmed axon pruning during *Drosophila* metamorphosis. Curr. Biol. *14*, 668–677.

Bagri, A., Cheng, H.J., Yaron, A., Pleasure, S.J., and Tessier-Lavigne, M. (2003). Stereotyped pruning of long hippocampal axon branches triggered by retraction inducers of the semaphorin family. Cell *113*, 285–299.

Beirowski, B., Adalbert, R., Wagner, D., Grumme, D.S., Addicks, K., Ribchester, R.R., and Coleman, M.P. (2005). The progressive nature of Wallerian degeneration in wild-type and slow Wallerian degeneration (WldS) nerves. BMC Neurosci. *6*, 6 10.1186/1471-2202-6-6.

Berdnik, D., Chihara, T., Couto, A., and Luo, L. (2006). Wiring stability of the adult *Drosophila* olfactory circuit after lesion. J. Neurosci. *26*, 3367–3376.

Bishop, D.L., Misgeld, T., Walsh, M.K., Gan, W.B., and Lichtman, J.W. (2004). Axon branch removal at developing synapses by axosome shedding. Neuron *44*, 651–661.

Cherbas, L., Hu, X., Zhimulev, I., Belyaeva, E., and Cherbas, P. (2003). EcR isoforms in *Drosophila*: testing tissue-specific requirements by targeted blockade and rescue. Development *130*, 271–284.

Conforti, L., Tarlton, A., Mack, T.G., Mi, W., Buckmaster, E.A., Wagner, D., Perry, V.H., and Coleman, M.P. (2000). A Ufd2/D4Cole1e chimeric protein and overexpression of Rbp7 in the slow Wallerian degeneration (WldS) mouse. Proc. Natl. Acad. Sci. USA *97*, 11377–11382.

DiAntonio, A., Haghighi, A.P., Portman, S.L., Lee, J.D., Amaranto, A.M., and Goodman, C.S. (2001). Ubiquitination-dependent mechanisms regulate synaptic growth and function. Nature *412*, 449–452.

Ferri, A., Sanes, J.R., Coleman, M.P., Cunningham, J.M., and Kato, A.C. (2003). Inhibiting axon degeneration and synapse loss attenuates apoptosis and disease progression in a mouse model of motoneuron disease. Curr. Biol. *13*, 669–673.

Freeman, M.R., Delrow, J., Kim, J., Johnson, E., and Doe, C.Q. (2003). Unwrapping glial biology. Gcm target genes regulating glial development, diversification, and function. Neuron *38*, 567–580.

Glass, J.D., Brushart, T.M., George, E.B., and Griffin, J.W. (1993). Prolonged survival of transected nerve fibres in C57BL/Ola mice is an intrinsic characteristic of the axon. J. Neurocytol. *22*, 311–321.

Griffin, J.W., George, E.B., Hsieh, S.-T., and Glass, J.D. (1995). Axonal degeneration and disorders of the axonal cytoskeleton. In The Axon: Structure, Function and Pathophysiology, S.G. Waxman, J.D. Kocsis, and P.K. Sytys, eds. (New York: Oxford University Press), pp. 375–390.

Innocenti, G.M., Clarke, S., and Koppel, H. (1983a). Transitory macrophages in the white matter of the developing visual cortex. II. Development and relations with axonal pathways. Brain Res. *313*, 55–66.

Innocenti, G.M., Koppel, H., and Clarke, S. (1983b). Transitory macrophages in the white matter of the developing visual cortex. I. Light and electron microscopic characteristics and distribution. Brain Res. *313*, 39–53.

Kuo, C.T., Jan, L.Y., and Jan, Y.N. (2005). Dendrite-specific remodeling of *Drosophila* sensory neurons requires matrix metalloproteases, ubiquitin-proteasome, and ecdysone signaling. Proc. Natl. Acad. Sci. USA *102*, 15230–15235.

Lee, T., and Luo, L. (1999). Mosaic analysis with a repressible cell marker for studies of gene function in neuronal morphogenesis. Neuron *22*, 451–461.

Lee, T., Lee, A., and Luo, L. (1999). Development of the *Drosophila* mushroom bodies: sequential generation of three distinct types of neurons from a neuroblast. Development *126*, 4065–4076.

Lee, T., Marticke, S., Sung, C., Robinow, S., and Luo, L. (2000). Cell-autonomous requirement of the USP/EcR-B ecdysone receptor for mushroom body neuronal remodeling in *Drosophila*. Neuron *28*, 807–818.

Liu, X.B., Low, L.K., Jones, E.G., and Cheng, H.J. (2005). Stereotyped axon pruning via plexin signaling is associated with synaptic complex elimination in the hippocampus. J. Neurosci. *25*, 9124–9134.

Lunn, E.R., Perry, V.H., Brown, M.C., Rosen, H., and Gordon, S. (1989). Absence of Wallerian degeneration does not hinder regeneration in peripheral nerve. Eur. J. Neurosci. *1*, 27–33.

Luo, L., and O'Leary, D.D.M. (2005). Axon retraction and degeneration in development and disease. Annu. Rev. Neurosci. *28*, 127–156.

MacDonald, J.M., Beach, M.G., Porpiglia, E., Sheehan, A.E., Watts, R.J., and Freeman, M.R. (2006). The *Drosophila* cell corpse engulfment receptor Draper mediates glial clearance of severed axons. Neuron *50*, this issue, 869–881.

Mack, T.G., Reiner, M., Beirowski, B., Mi, W., Emanuelli, M., Wagner, D., Thomson, D., Gillingwater, T., Court, F., Conforti, L., et al. (2001). Wallerian degeneration of injured axons and synapses is delayed by a Ube4b/Nmnat chimeric gene. Nat. Neurosci. *4*, 1199–1206.

Marin, E.C., Watts, R.J., Tanaka, N.K., Ito, K., and Luo, L. (2005). Developmentally programmed remodeling of the *Drosophila* olfactory circuit. Development *132*, 725–737.

McLaughlin, T., and O'Leary, D.D.M. (2005). Molecular gradients and development of retinotopic maps. Annu. Rev. Neurosci. *28*, 327–355.

McLaughlin, T., Torborg, C.L., Feller, M.B., and O'Leary, D.D.M. (2003). Retinotopic map refinement requires spontaneous retinal waves during a brief critical period of development. Neuron *18*, 1147–1160.

Mi, W., Beirowski, B., Gillingwater, T.H., Adalbert, R., Wagner, D., Grumme, D., Osaka, H., Conforti, L., Arnhold, S., Addicks, K., et al. (2005). The slow Wallerian degeneration gene, WldS, inhibits axonal spheroid pathology in gracile axonal dystrophy mice. Brain *128*, 405–416.

Nakamura, H., and O'Leary, D.D.M. (1989). Inaccuracies in initial growth and arborization of chick retinotectal axons followed by course corrections and axon remodeling to develop topographic order. J. Neurosci. *9*, 3776–3795.

O'Leary, D.D.M., and Terashima, T. (1988). Cortical axons branch to multiple subcortical targets by interstitial axon budding: implications for target recognition and "waiting periods". Neuron *1*, 901–910.

O'Leary, D.D.M., Bicknese, A.R., De Carlos, J.A., Heffner, C.D., Koester, S.E., Kutka, L.J., and Terashima, T. (1990). Target selection by cortical axons: alternative mechanisms to establish axonal connections in the developing brain. Cold Spring Harb. Symp. Quant. Biol. *55*, 453–468.

Pak, W., Hindges, R., Lim, Y.-S., Pfaff, S.L., and O'Leary, D.D.M. (2004). Magnitude of binocular vision controlled by Islet-2 repression of a genetic program that specifies laterality of retinal axon pathfinding. Cell *119*, 567–578.

Parson, S.H., Mackintosh, C.L., and Ribchester, R.R. (1997). Elimination of motor nerve terminals in neonatal mice expressing a gene for slow Wallerian degeneration (C57Bl/Wlds). Eur. J. Neurosci. *9*, 1586–1592.

Portera-Cailliau, C., Weimer, R.M., De Paola, V., Caroni, P., and Svoboda, K. (2005). Diverse modes of axon elaboration in the developing neocortex. PLoS Biol. *3*, e272. 10.1371/journal.pbio.0030272.

Raff, M.C., Whitmore, A.V., and Finn, J.T. (2002). Axonal self-destruction and neurodegeneration. Science *296*, 868–871.

Sajadi, A., Schneider, B.L., and Aebischer, P. (2004). Wlds-mediated protection of dopaminergic fibers in an animal model of Parkinson disease. Curr. Biol. *14*, 326–330.

Samsam, M., Mi, W., Wessig, C., Zielasek, J., Toyka, K.V., Coleman, M.P., and Martini, R. (2003). The Wlds mutation delays robust loss of motor and sensory axons in a genetic model for myelin-related axonopathy. J. Neurosci. *23*, 2833–2839.

Schubiger, M., Tomita, S., Sung, C., Robinow, S., and Truman, J.W. (2003). Isoform specific control of gene activity in vivo by the *Drosophila* ecdysone receptor. Mech. Dev. *120*, 909–918.

Stocker, R.F., Lienhard, M.C., Borst, A., and Fischbach, K.-F. (1990). Neuronal architecture of the antennal lobe in *Drosophila melanogaster*. Cell Tissue Res. *262*, 9–34.

Stockinger, P., Kvitsiani, D., Rotkopf, S., Tirian, L., and Dickson, R.J. (2005). Neural circuitry that governs *Drosophila* male courtship behavior. Cell *121*, 795–807.

Vosshall, L.B., Wong, A.M., and Axel, R. (2000). An olfactory sensory map in the fly brain. Cell *102*, 147–159.

Waller, A. (1850). Experiments on the section of glossopharyngeal and hypoglossal nerves of the frog and observations of the alternatives produced thereby in the structure of their primitive fibers. Philos. Trans. R. Soc. Lond. B Biol. Sci. *140*, 423–429.

Wang, J., Zhai, Q., Chen, Y., Lin, E., Gu, W., McBurney, M.W., and He, Z. (2005). A local mechanism mediates NAD-dependent protection of axon degeneration. J. Cell Biol. *170*, 349–355.

Watts, R.J., Hoopfer, E.D., and Luo, L. (2003). Axon pruning during *Drosophila* metamorphosis: evidence for local degeneration and requirement of the ubiquitin-proteasome system. Neuron *38*, 871–885.

Watts, R.J., Schuldiner, O., Perrino, J., Larsen, C., and Luo, L. (2004). Glia engulf degenerating axons during developmental axon pruning. Curr. Biol., in press.

Williams, D.W., and Truman, J.W. (2005). Cellular mechanisms of dendrite pruning in *Drosophila*: insights from in vivo time-lapse of remodeling dendritic arborizing sensory neurons. Development *132*, 3631–3642.

Zhai, Q., Wang, J., Kim, A., Liu, Q., Watts, R., Hoopfer, E., Mitchison, T., Luo, L., and He, Z. (2003). Involvement of the ubiquitin-proteasome system in the early stages of wallerian degeneration. Neuron *39*, 217–225.

Zhou, Z., Hartwieg, E., and Horvitz, H.R. (2001). CED-1 is a transmembrane receptor that mediates cell corpse engulfment in C. elegans. Cell *104*, 43–56.